electronics

MDPI

Article

Multisource Power Splitting Energy Harvesting Relaying Network in Half-Duplex System over Block Rayleigh Fading Channel: System Performance Analysis

Tan N. Nguyen [1], Minh Tran [2,*], Thanh-Long Nguyen [3], Duy-Hung Ha [1] and Miroslav Voznak [1]

1 Faculty of Electrical Engineering and Computer Science, VSB-Technical University of Ostrava 17, listopadu 15/2172, 708 33 Ostrava-Poruba, Czech Republic; tan.nhat.nguyen.st@vsb.cz (T.N.N.); duy.hung.ha.st@vsb.cz (D.-H.H.); miroslav.voznak@vsb.cz (M.V.)

2 Optoelectronics Research Group, Faculty of Electrical and Electronics Engineering, Ton Duc Thang University, Ho Chi Minh City 70000, Vietnam

3 Center for Information Technology, Ho Chi Minh City University of Food Industry, Ho Chi Minh City 70000, Vietnam; longngth@gmail.com

* Correspondence: tranhoangquangminh@tdtu.edu.vn; Tel.: +84-28-377-55-028

Received: 2 November 2018; Accepted: 2 January 2019; Published: 7 January 2019

Abstract: Energy harvesting and information transferring simultaneously by radio frequency (RF) is considered as the novel solution for green-energy wireless communications. From that point of view, the system performance (SP) analysis of multisource power splitting (PS) energy harvesting (EH) relaying network (RN) over block Rayleigh-fading channels is presented and investigated. We investigate the system in both delay-tolerant transmission (DTT), and delay-limited transmission (DLT) modes and devices work in the half-duplex (HD) system. In this model system, the closed-form (CF) expressions for the outage probability (OP), system throughput (ST) in DLT mode and for ergodic capacity (EC) for DTT mode are analyzed and derived, respectively. Furthermore, CF expression for the symbol errors ratio (SER) is demonstrated. Then, the optimal PS factor is investigated. Finally, a Monte Carlo simulation is used for validating the analytical expressions concerning with all system parameters (SP).

Keywords: power splitting (PS); energy harvesting (EH); relaying network (RN); system performance (SP); half-duplex (HD)

1. Introduction

Conventionally, wireless devices are powered by batteries, which have a limited operational lifetime, and have to be replaced or recharged periodically to maintain the network connectivity. In practice, this could be costly, inconvenient, and even infeasible. To overcome the above limitation, there have been several research ideas on microwave-enabled wireless energy transfer (WET), where energy is continuously and stably supplied over the air. More advancing, the WET technologies to power the devices efficiently open up the potential to build a fully wireless powered communication network (WPCN), in which wireless devices communicate using only the power harvested by means of WET [1–3]. In a wireless network, the source (S) and destination (D) may not communicate with each other directly because the distance between S and D is more significant in comparison with their transmission range. Then, the intermediate relay (R) node is necessary for this communication purpose, which can reduce the shadowing, fading, and path loss in communication network [1–4].

In relay networks (RN), R helps to exchange the information radio signal between S and D with or without decoding. In a typical way, powered wireless communication devices by batteries with a limited operational lifetime, and be replaced or recharged periodically is popularly used. In practice, this operation could be inconvenient, costly and even infeasible. In particular, because of the critical role of relays, the energy problem becomes vital in wireless relay networks. So far, there are many solutions for improving energy efficiency at the relay nodes, for example in [5–7]. While being powered by batteries is the standard way to harvest energy by conventional wireless devices, radio-frequency (RF) signals can, continuously and in a stable manner, transfer energy over the air by energy harvesting wireless networks [6–9]. Furthermore, the relaying network can solve the energy saving problem and can be considered as a novel approach for applying EH to the relay network [10–13].

In the last decade, EH and information transferring (IT) using a RF signal was proposed and intensively studied. We can see that EH and IT are deeply investigated in [7–9]. For simultaneous EH and IT processes, dynamic power splitting (PS) schemes including PS and time switching (TS) were presented in [14–16]. Furthermore, the influence of the PS factor on the ergodic capacity for IT and EH is proposed and investigated in [17,18]. From that point of view, an EH relaying network (RN) is necessary to be further investigated in several kinds of literature. As an example, the authors of [19–21] analyzed a three-node model with an EH relay in both PS and TS protocols. Moreover, refs. [22–24] extended previous works by investigating multiple EH relays in both amplify-and-forward (AF) and decode-and-forward (DF) protocols. After that, refs. [25,26] presented and discussed the multiple EH relays and a two-way EH RN. Also, refs. [27,28] proposed the direct link and the relaying links model in different modes, in which the relaying links are used only when the direct link was not enough for covering the transmission process. From that point of view, research in EH relaying network is still open and exciting for both academic and industrial purposes.

The primary purpose of this article is to provide a system performance (SP) analysis of a multisource PS EH relaying network in the half-duplex (HD) mode over a block Rayleigh-fading channel in both DLT and DTT modes. In the analysis process, we analyzed and derived the closed-form (CF) expressions of the outage probability (OP) and system throughput (ST) in DLT mode and a CF expression for ergodic capacity (EC) for DTT mode, respectively. Furthermore, we can obtain the CF expression for symbol errors ratio (SER) for DLT mode. After that, the optimal PS factor is investigated and derived in details. Finally, the Monte Carlo simulation is used for validating the analytical analysis in connection with all system parameters. The main contributions of this research can be focused as:

(1) We present and investigate SP analysis of multisource PS EH relaying network in the HD mode over block Rayleigh-fading channel in both DLT and DTT modes.
(2) The CF expressions of the OP for DLT mode and EC for DTT mode are proposed, analyzed and derived.
(3) The CF for SER for DLT mode is analyzed and derived.
(4) The influence of all primary system parameters on OP, EC, and SER is investigated and discussed.
(5) All research results are demonstrated using the Monte Carlo simulation.

The rest of this manuscript is as follows: Firstly, we present the proposed system model in Section 2; Section 3 investigates the system performance of the system model; Numerical results and some discussion are drawn in Section 4. Some conclusions of this manuscript are proposed in Section 5.

2. System Model

In this section, an EH relaying network with multisource (S), destination (D) and one relay (R) as shown in Figure 1. The model system works along the principles of analog coding network [29–31]. In Figure 1, S, R and D have only one antenna and operate in HD mode. The channel gains between S_n and R and between R and D are denoted a h_{SnD} and h_{RD}, which are Rayleigh fading channels. In this model, we consider that the S_n and D direct link is fragile, and they can communicate with each other via the R helping relay. Moreover, R has only the energy enough for its purpose, so R needs to harvest

the energy from S before forwarding the information messages to D. Commonly, we assume that S and D, as well as R, know the channel gains. The EH and IT processes for the model system is illustrated in Figure 2. In this protocol, each transmission block time T divides of two time slots. In the first-half time slot $T/2$, R harvests energy ρPSn and receives information $(1-\rho)P_{sn}$ from S_n. The remaining half-time slot $T/2$ are used for IT process from R to D after R amplifies the signal that it received [29,30].

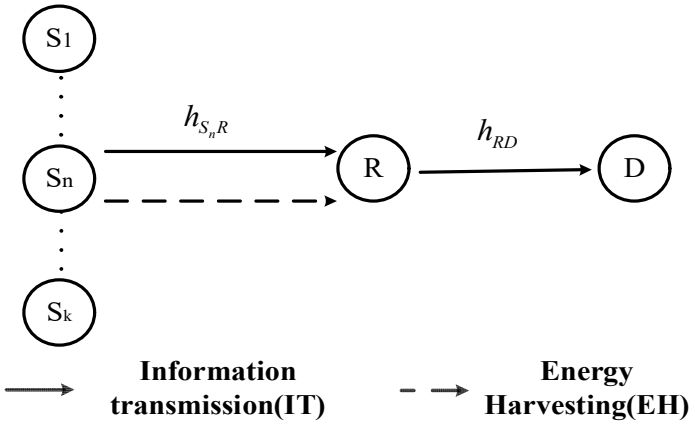

Figure 1. System model.

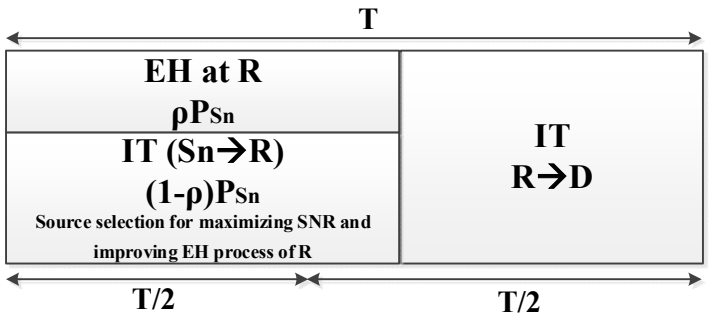

Figure 2. Energy harvesting (EH) and Information transmission (IT) processes with PS relaying protocol.

3. The System Performance

Suppose that source S_n is chosen to perform the EH and IT processes to R. In the first stage, R receive the signal as

$$y_r = \sqrt{(1-\rho)}h_{S_nR}x_{s_n} + n_r, \tag{1}$$

where h_{S_nR} is S_n to R channel gain, and $n \in (1, 2, \ldots, K)$.

Here, x_{S_n} is the transmitted signal at S, n_r is the additive white Gaussian noise (AWGN) with variance N_0 and $0 < \rho < 1$ is PS ratio at R. Here $E\left\{|x_{S_n}|^2\right\} = P_{S_n}$, $E\{\bullet\}$ is expectation operator, and P_{S_n} is average transmit power at S_n.

The harvested power at R is obtained as

$$P_r = \frac{E_h}{T/2} = \frac{\eta\rho P_{S_n}|h_{S_nR}|^2(T/2)}{T/2} = \eta\rho P_{S_n}|h_{S_nR}|^2, \tag{2}$$

where $0 < \eta \leq 1$ is energy conversion efficiency of EH at R.

The received signal at D is formulated as the below equation

$$y_D = h_{RD}x_r + n_D, \tag{3}$$

where h_{RD} is R to D channel gain, n_D is AWGN with variance N_0, and $E\left\{|x_r|^2\right\} = P_r$.

3.1. Delay-Limited Transmission (DLT) Mode

In the AF protocol, the signal transmitted by R is an amplified version of y_r [21]

$$\beta = \frac{x_r}{y_r} = \sqrt{\frac{P_r}{\eta\rho P_{S_n}|h_{S_nR}|^2 + N_0}}, \tag{4}$$

where β is the amplifying factor at R.

From (1), (3) and (4), D receives signal in the second time slot can be calculated as

$$\begin{aligned} y_D &= h_{RD}\beta y_r + n_D = h_{RD}\beta\left[\sqrt{(1-\rho)}h_{S_nR}x_{S_n} + n_r\right] + n_D \\ &= \underbrace{\sqrt{(1-\rho)}h_{S_nR}x_{S_n}h_{RD}\beta}_{signal} + \underbrace{h_{RD}\beta n_r + n_D}_{noise}. \end{aligned} \tag{5}$$

The overall signal to noise ratio (SNR) from S to D can be formulated by the following

$$SNR_{AF} = \frac{\mathrm{E}\left\{|signal|^2\right\}}{\mathrm{E}\left\{|noise|^2\right\}} = \frac{(1-\rho)P_s|h_{S_nR}|^2|h_{RD}|^2\beta^2}{|h_{RD}|^2\beta^2N_0 + N_0} = \frac{(1-\rho)P_s|h_{S_nR}|^2|h_{RD}|^2}{|h_{RD}|^2N_0 + \frac{N_0}{\beta^2}}. \tag{6}$$

By doing some algebra and using the fact that $N_0 << P_r$, (6) can be reformulated as

$$SNR_{AF} = \frac{(1-\rho)P_{S_n}P_r|h_{S_nR}|^2|h_{RD}|^2}{|h_{RD}|^2P_rN_0 + (1-\rho)P_{S_n}|h_{S_nR}|^2N_0}. \tag{7}$$

Combine with (2), we have:

$$SNR_{AF} = \frac{\eta\rho(1-\rho)\psi|h_{S_nR}|^2|h_{RD}|^2}{\eta\rho|h_{RD}|^2 + (1-\rho)}. \tag{8}$$

Here, we denote that $\psi = P_{S_n}/N_0$.

Remark 1. *The best source S_{n^*} would be selected to maximize the received SNR at D to optimize the transmission performance, then we have*

$$n^* = \arg\max_{1\le n\le K}[SNR_{AF}]. \tag{9}$$

In this analysis, the optimal source selection protocol in which the best selection source is selected as follows

$$\omega_1 = \max_{n=1,2,\ldots,K}(|h_{S_nR}|^2). \tag{10}$$

In [32], the cumulative distribution function (CDF) of ω_1 is given by the following

$$F_{\omega_1}(y) = \sum_{p=0}^{K}(-1)^pC_K^p \times e^{-py/\lambda_1}, \tag{11}$$

where λ_1 is the mean of random variable (RV) ω_1, and $C_K^p = \frac{K!}{p!(K-p)!}$.

Then, the corresponding probability density function (PDF) can be obtained by the below equation

$$f_{\omega_1}(y) = \frac{1}{\lambda_1}\sum_{p=0}^{K-1}(-1)^pC_{K-1}^pK \times e^{-(p+1)y/\lambda_1}. \tag{12}$$

Proposition 1. *The outage probability (OP) of the model system can be calculated by*

$$\begin{aligned} OP_{AF} &= \Pr(SNR_{AF} < \gamma_{th}) = \Pr\left[\frac{\eta\rho(1-\rho)\psi \max\left\{\left|h_{S_nR}\right|^2\right\}|h_{RD}|^2}{\eta\rho|h_{RD}|^2+(1-\rho)} < \gamma_{th}\right] \\ &= \Pr\left[\frac{\eta\rho(1-\rho)\psi\omega_1\omega_2}{\eta\rho\omega_2+(1-\rho)} < \gamma_{th}\right] = \Pr[\eta\rho\omega_2\{(1-\rho)\psi\omega_1 - \gamma_{th}\} < \gamma_{th}(1-\rho)] \\ &= \begin{cases} \Pr\left[\omega_2 < \frac{\gamma_{th}(1-\rho)}{\eta\rho\{(1-\rho)\psi\omega_1-\gamma_{th}\}}\right], \omega_1 > \frac{\gamma_{th}}{(1-\rho)\psi} \\ 1, \omega_1 \le \frac{\gamma_{th}}{(1-\rho)\psi} \end{cases}, \end{aligned} \tag{13}$$

where $\gamma_{th} = 2^{2R} - 1$ *is a threshold, and R is source rate of the proposed system model.*

Equation (13) can be computed as the following

$$OP_{AF} = \int_0^{\frac{\gamma_{th}}{(1-\rho)\psi}} f_{\omega_1}(\omega_1)d\omega_1 + \int_{\frac{\gamma_{th}}{(1-\rho)\psi}}^{\infty} F_{\omega_2}\left[\frac{\gamma_{th}(1-\rho)}{\eta\rho\{(1-\rho)\psi\omega_1 - \gamma_{th}\}}\right] f_{\omega_1}(\omega_1)d\omega_1, \tag{14}$$

$$OP_{AF} = 1 - \frac{1}{\lambda_1}\int_{\frac{\gamma_{th}}{(1-\rho)\psi}}^{\infty} \sum_{p=0}^{M-1} (-1)^p C_{M-1}^p M \times e^{-(p+1)\omega_1/\lambda_1} \times e^{-\frac{\gamma_{th}(1-\rho)}{\eta\rho\{(1-\rho)\psi\omega_1-\gamma_{th}\}\lambda_2}} d\omega_1. \tag{15}$$

By changing variable $t = (1-\rho)\psi\omega_1 - \gamma_{th}$ into Equation (15), it can be rewritten as the following

$$OP_{AF} = 1 - \frac{1}{(1-\rho)\psi\lambda_1}\sum_{p=0}^{K-1} (-1)^p C_{K-1}^p K \times e^{-\frac{(p+1)\gamma_{th}}{(1-\rho)\psi\lambda_1}} \times \int_0^{\infty} e^{-\frac{(p+1)t}{(1-\rho)\psi\lambda_1}} \times e^{-\frac{\gamma_{th}(1-\rho)}{\eta\rho t\lambda_2}} dt. \tag{16}$$

Applying the table of integral eq (3.324,1) in [33], Equation (16) can be reformulated as

$$OP_{AF} = 1 - 2\sum_{p=0}^{K-1} (-1)^p C_{K-1}^p K \times e^{-\frac{(p+1)\gamma_{th}}{(1-\rho)\psi\lambda_1}} \times \sqrt{\frac{\gamma_{th}}{\eta\rho\psi(p+1)\lambda_1\lambda_2}} \times K_1\left[2\sqrt{\frac{\gamma_{th}(p+1)}{\eta\rho\psi\lambda_1\lambda_2}}\right], \tag{17}$$

where $K_v(\bullet)$ is the modified Bessel function of the second kind and v$^{\text{th}}$ order.

Proposition 2. *The throughput of system model can be formulated as*

$$\begin{aligned} \tau &= (1 - OP_{AF})\frac{R(T/2)}{T} = (1 - OP_{AF})\frac{R}{2} \\ &= \sum_{p=0}^{K-1} (-1)^p C_{K-1}^p K \times R \times e^{-\frac{(p+1)\gamma_{th}}{(1-\rho)\psi\lambda_1}} \times \sqrt{\frac{\gamma_{th}}{\eta\rho\psi(p+1)\lambda_1\lambda_2}} \times K_1\left[2\sqrt{\frac{\gamma_{th}(p+1)}{\eta\rho\psi\lambda_1\lambda_2}}\right]. \end{aligned} \tag{18}$$

3.2. Delay-Tolerant Transmission (DTT) Mode

Using the received SNR at D, SNR_{AF} in (8), C is given by the following

$$C = \text{E}_{h_{S_nR}, h_{RD}}\{\log_2(1 + SNR_{AF})\}. \tag{19}$$

Proposition 3. *The ergodic capacity (EC) at the destination node is formulated like Equation (25) in* [31] *by the following*

$$C = \int_{\gamma=0}^{\infty} f_{SNR_{AF}}(\gamma)\log_z(1+\gamma)d\gamma = \frac{1}{\ln 2}\int_0^{\infty} \frac{1 - F_{SNR_{AF}}(\gamma)}{1+\gamma}d\gamma. \tag{20}$$

In (20), we denote

$$F_{SNR_{AF}}(\gamma) = 1 - 2\sum_{p=0}^{K-1}(-1)^p C_{K-1}^{p} K \times e^{-\frac{(p+1)\gamma}{(1-\rho)\psi\lambda_1}} \times \sqrt{\frac{\gamma}{\eta\rho\psi(p+1)\lambda_1\lambda_2}} \times K_1\left[2\sqrt{\frac{\gamma(p+1)}{\eta\rho\psi\lambda_1\lambda_2}}\right]. \quad (21)$$

We can observe that the involving integral in (18) is complicated to be solved in CF. However, by changing the variable of the integration in (16) as $\gamma = \tan\theta$, Equation (20) can be rewritten as the below equation

$$C = \frac{1}{\ln 2}\int_0^{\infty} \frac{1 - F_{SNR_{AF}}(\gamma)}{1+\gamma} d\gamma = \frac{1}{\ln 2}\int_0^{\pi/2} \frac{1 - F_{SNR_{AF}}(\tan\theta)}{1+\tan\theta} \sec^2\theta d\theta. \quad (22)$$

Furthermore, we can apply an efficient NP-point Gauss–Chebychev quadrature (GCQ) formula as in [34] to numerically derive as

$$C = \frac{1}{\ln 2}\sum_{v=1}^{N_p} \varphi_v \frac{1 - F_{SNR_{AF}}(x_v)}{1+x_v}, \quad (23)$$

where we denote that $x_v = \tan\left(\frac{\pi}{4}\cos\left[\frac{2v-1}{2N_p}\pi\right] + \frac{\pi}{4}\right)$ and $\varphi_v = \frac{\pi^2 \sin\left(\frac{2v-1}{2N_p}\pi\right)}{4N_p \cos^2\left(\frac{\pi}{4}\cos\left[\frac{2v-1}{2N_p}\pi\right]+\frac{\pi}{4}\right)}$.

3.3. Symbol Error Ratio (SER) Analysis

For obtaining novel SER expression at D, the OP in [35] can be considered as the first stage, and the equation for SER can formulate as below

$$SER = \mathrm{E}\left[aQ(\sqrt{2b(SNR_{AF})}\right], \quad (24)$$

where $Q(t) = \frac{1}{\sqrt{2\pi}}\int_t^{\infty} e^{-x^2/2}dx$ is the Gaussian Q-function, a and b are constants with binary phase-shift keying (BPSK) $(a,b) = (1,1)$ for BPSK; $(a,b) = (1,2)$ for Quadrature Phase Shift Keying (QPSK) and binary frequency-shift keying (BFSK) with orthogonal signaling $(a,b) = (1,0.5)$ or minimum correlation $(a,b) = (1,0.715)$. As a result, the SER expression is given in (25) directly regarding OP at S by using integration, as follows

$$SER = \frac{a\sqrt{b}}{2\sqrt{\pi}}\int_0^{\infty} \frac{e^{-bx}}{\sqrt{x}} F_{SNR_{AF}}(x)dx. \quad (25)$$

Substituting (21) into (25) and replace $\gamma = x$, we obtain the following expression

$$\begin{aligned} SER &= \frac{a\sqrt{b}}{2\sqrt{\pi}}\int_0^{\infty} \frac{e^{-bx}}{\sqrt{x}}\left[1 - 2\sum_{p=0}^{K-1}(-1)^p C_{K-1}^{p} K \times e^{-\frac{(p+1)x}{(1-\rho)\psi\lambda_1}} \times \sqrt{\frac{x}{\eta\rho\psi(p+1)\lambda_1\lambda_2}} \times K_1\left[2\sqrt{\frac{x(p+1)}{\eta\rho\psi\lambda_1\lambda_2}}\right]\right]dx \\ &= \frac{a\sqrt{b}}{2\sqrt{\pi}}\int_0^{\infty} \frac{e^{-bx}}{\sqrt{x}}dx - \frac{a\sqrt{b}}{\sqrt{\pi}}\sum_{p=0}^{K-1}(-1)^p C_{K-1}^{p} \frac{K}{\sqrt{\eta\rho\psi(p+1)\lambda_1\lambda_2}} \times \int_0^{\infty} e^{-x\left[b+\frac{(p+1)}{(1-\rho)\psi\lambda_1}\right]} \times K_1\left[2\sqrt{\frac{x(p+1)}{\eta\rho\psi\lambda_1\lambda_2}}\right]dx, \end{aligned} \quad (26)$$

where we denote that $J_1 = \frac{a\sqrt{b}}{2\sqrt{\pi}}\int_0^{\infty} \frac{e^{-bx}}{\sqrt{x}}dx$.

Applying eq (3.361,2) in [33], and $J_1 = \frac{a}{2}$, we denote J_2 as the following

$$J_2 = \frac{a\sqrt{b}}{\sqrt{\pi}} \sum_{p=0}^{K-1} (-1)^p C_{K-1}^p \frac{K}{\sqrt{\eta\rho\psi(p+1)\lambda_1\lambda_2}} \times \int_0^\infty e^{-x\left[b+\frac{(p+1)}{(1-\rho)\psi\lambda_1}\right]} \times K_1\left[2\sqrt{\frac{x(p+1)}{\eta\rho\psi\lambda_1\lambda_2}}\right] dx. \quad (27)$$

Applying eq (6.614,5) in [33], J_2 can be reformulated as

$$J_2 = \frac{a\sqrt{b}}{\sqrt{\pi}} \sum_{p=0}^{K-1} (-1)^p C_{K-1}^p \frac{K}{\sqrt{\eta\rho\psi(p+1)\lambda_1\lambda_2}} \times \int_0^\infty e^{-x\left[b+\frac{(p+1)}{(1-\rho)\psi\lambda_1}\right]} \times K_1\left[2\sqrt{\frac{x(p+1)}{\eta\rho\psi\lambda_1\lambda_2}}\right] dx, \quad (28)$$

$$\begin{aligned} J_2 &= \tfrac{a\sqrt{b}}{4} \sum_{p=0}^{K-1} (-1)^p C_{K-1}^p \tfrac{K}{\eta\rho\psi\lambda_1\lambda_2} \times \frac{1}{\sqrt{\left[b+\frac{(p+1)}{(1-\rho)\psi\lambda_1}\right]^3}} \times \exp\left[\tfrac{(p+1)(1-\rho)}{2\eta\rho\lambda_2\{b(1-\rho)\psi\lambda_1+(p+1)\}}\right] \\ &\times \left\langle K_1\left[\tfrac{(p+1)(1-\rho)}{2\eta\rho\lambda_2\{b(1-\rho)\psi\lambda_1+(p+1)\}}\right] - K_0\left[\tfrac{(p+1)(1-\rho)}{2\eta\rho\lambda_2\{b(1-\rho)\psi\lambda_1+(p+1)\}}\right] \right\rangle. \end{aligned} \quad (29)$$

Finally, SER can be rewritten as the below equation

$$\begin{aligned} SER &= \tfrac{a}{2} - \tfrac{a\sqrt{b}}{4} \sum_{p=0}^{K-1} (-1)^p C_{K-1}^p \tfrac{K}{\eta\rho\psi\lambda_1\lambda_2} \times \frac{1}{\sqrt{\left[b+\frac{(p+1)}{(1-\rho)\psi\lambda_1}\right]^3}} \times \exp\left[\tfrac{(p+1)(1-\rho)}{2\eta\rho\lambda_2\{b(1-\rho)\psi\lambda_1+(p+1)\}}\right] \\ &\times \left\langle K_1\left[\tfrac{(p+1)(1-\rho)}{2\eta\rho\lambda_2\{b(1-\rho)\psi\lambda_1+(p+1)\}}\right] - K_0\left[\tfrac{(p+1)(1-\rho)}{2\eta\rho\lambda_2\{b(1-\rho)\psi\lambda_1+(p+1)\}}\right] \right\rangle \end{aligned} \quad (30)$$

3.4. Optimal Power Splitting Factor

In this paper, the optimal PS factor can be formulated by solving the equation $\frac{d\tau}{d\rho} = 0$. Here, we apply an iterative algorithm to solve this problem numerically. In particular, the Golden section search algorithm, which has been used in many global optimization problems in communications (for example, in [36]), is chosen for this work. For a detailed algorithm as well as its related theory, please refer to [37].

4. Numerical Results and Discussion

For validation, the correctness of the derived SP expressions, as well as investigation of the effect of all primary parameters on the SP, a set of Monte Carlo simulations are conducted and presented in this section [29–32]. All main simulation parameters are listed in Table 1.

Table 1. Simulation parameters.

Symbol	Name	Values
η	Energy harvesting efficiency	0.8
λ_1	Mean of $\left\|h_{S_nR}\right\|^2$	0.5
λ_2	Mean of $\left\|h_{RD}\right\|^2$	0.5
γ_{th}	SNR threshold	1
P_s/N_0	Source power to noise ratio	0–20 dB
R	Source rate	0.5 bit/s/Hz
K	Number of sources	1–10

4.1. Delay-Limited Transmission (DLT) Analysis

We first show the OP and ST of the DTT mode versus the PS factor ρ with R = 0.5 bps, η = 0.8, P_s/N_0 = 10 dB and K = 1, 3, 5 (Figures 3 and 4). As can be seen from Figures 3 and 4, the theoretical curves match to the simulated ones. Figure 3 shows that the OP firstly decreases when ρ increases from 0 to 0.6 and then has a massive increase with ρ from 0.6 to 1. In a contraction, the ST has a

remarkable increase in the first interval ρ from 0 to 0.6 and then decreases after optimal value ρ. It can be formulated that less available power for EH in the interval of ρ smaller than the optimal ρ leads to less transmission power from the relay node and smaller values of throughput are observed at the destination node and larger outage probability. On another way, the wasted power on EH in EH and less power is left for the source to relay information transmission leads to poor signal strength at the relay node, larger outage and lesser throughput at the destination node.

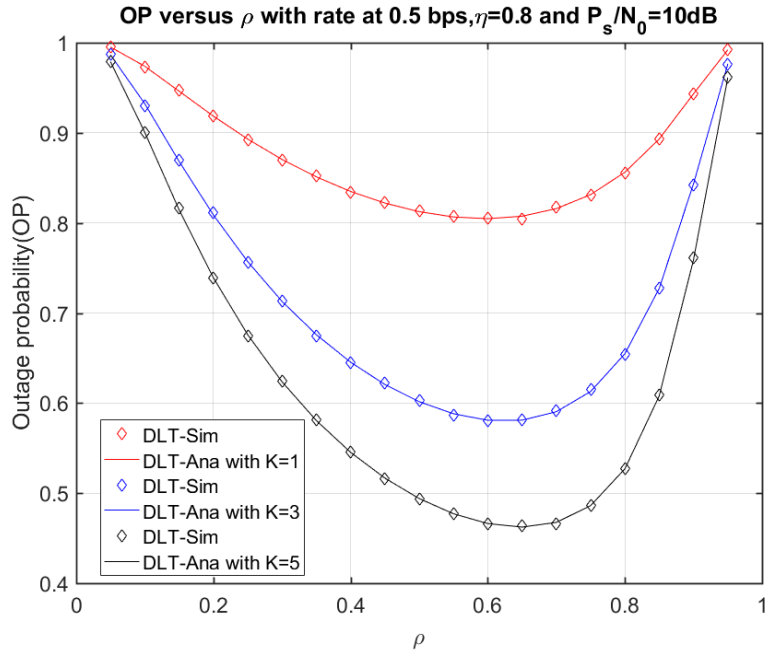

Figure 3. Outage Probability (OP) versus ρ with R = 0.5 bps, η = 0.8, P_s/N_0 = 10 dB and K = 1, 3, 5.

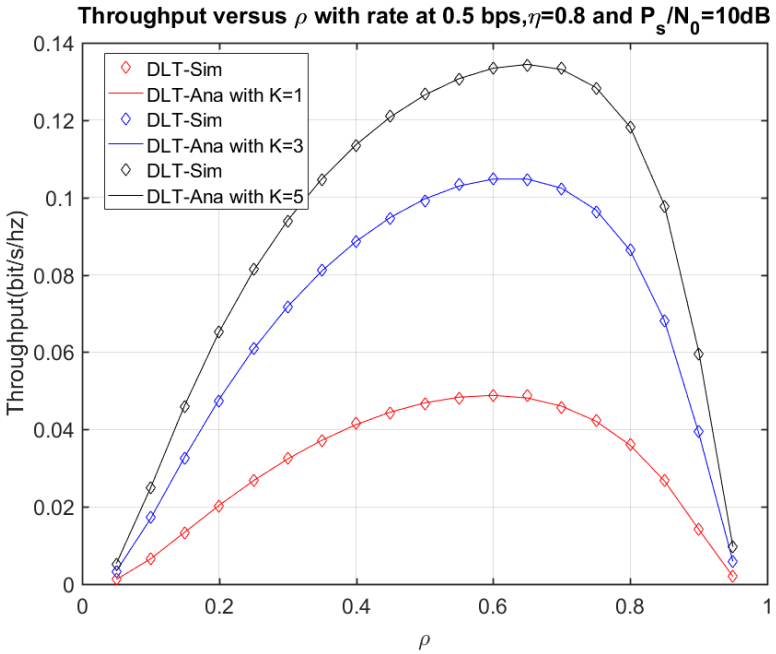

Figure 4. System Throughput (ST) versus ρ with R = 0.5 bps, η = 0.8, P_s/N_0 = 10 dB and K = 1, 3, 5.

Figures 5 and 6 depict the OP and ST of the model system versus energy conversion efficiency η for ρ = 0.5, K = 2, P_s/N_0 = 10 dB and R = 0.5, 1, 1.5. In these figures, the OP decreases and the ST

increases while η varies from 0 to 1. The results show that the case with R = 0.5 is the best case in comparison with the other cases in both outage probability and system throughput. Furthermore, all the analytical results are validated by the Monte Carlo simulation. It can be observed that the more efficacy of EH at the relay node, the higher ST and smaller OT of the proposed system.

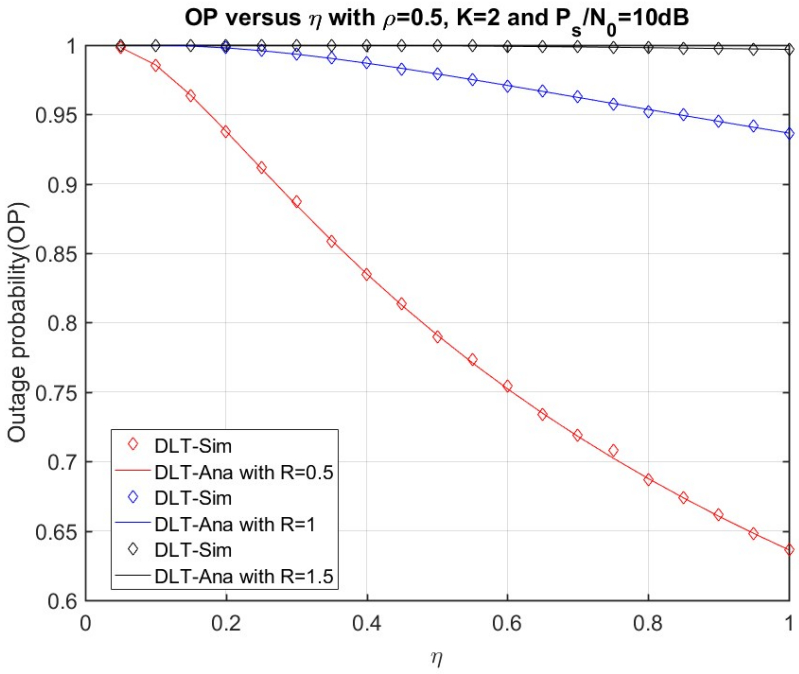

Figure 5. OP versus η for ρ = 0.5, K = 2, P_s/N_0 = 10 dB and R = 0.5, 1, 1.5.

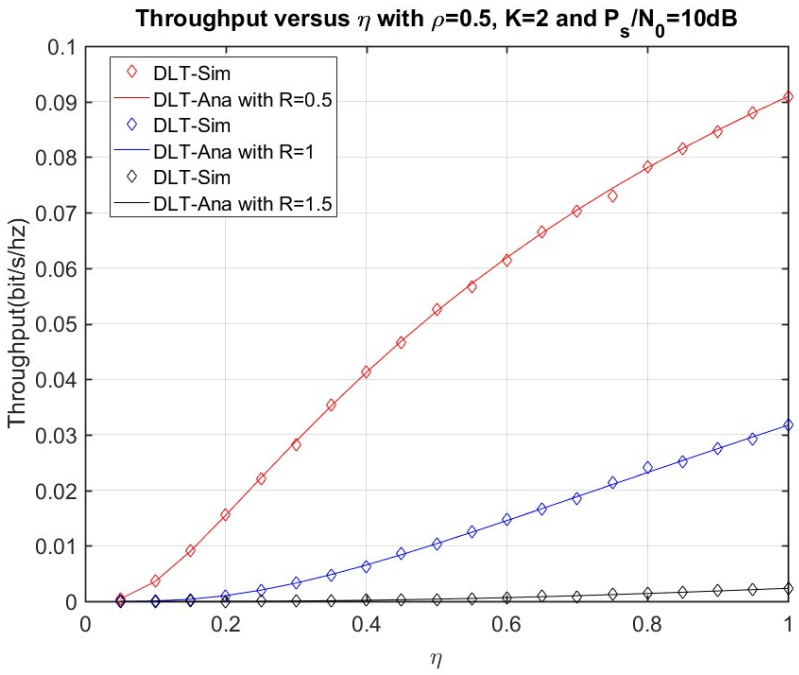

Figure 6. ST versus η for ρ = 0.5, K = 2, P_s/N_0 = 10 dB and R = 0.5, 1, 1.5.

Figures 7 and 8 plot the OP and ST concerning P_s/N_0. In this Figs, we set the main parameters as η = 0.8, R = 0.5 bps K = 2 and ρ = 0.2, 0.5, 0.7. From the results, we can see that the exact OP decreases and the ST increase when the ratio P_s/N_0 increases from 0 to 20 dB. From Figures 7 and 8, the analytical results and the simulation results match well with each other for all P_s/N_0.

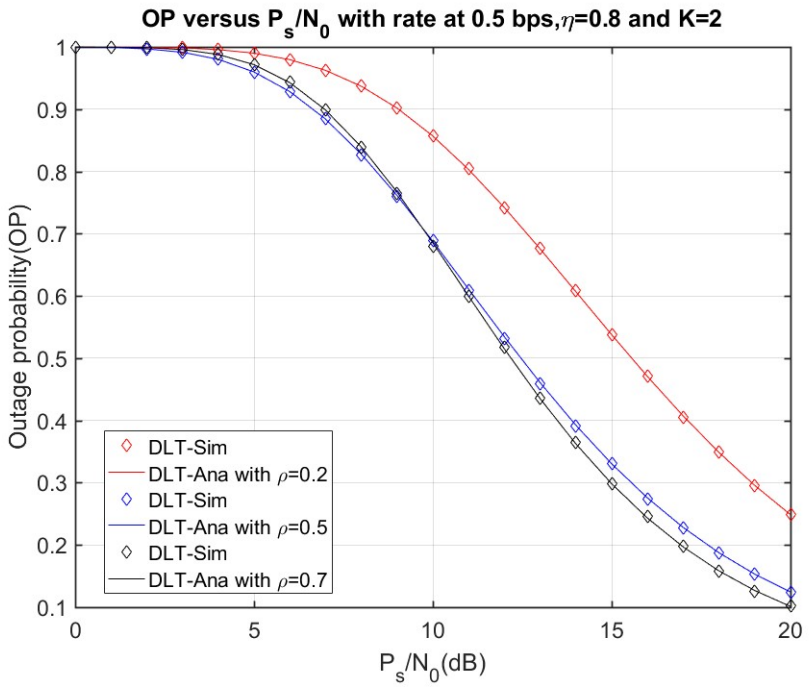

Figure 7. OP versus P_s/N_0 as η = 0.8, R = 0.5 bps K = 2 and ρ = 0.2, 0.5, 0.7.

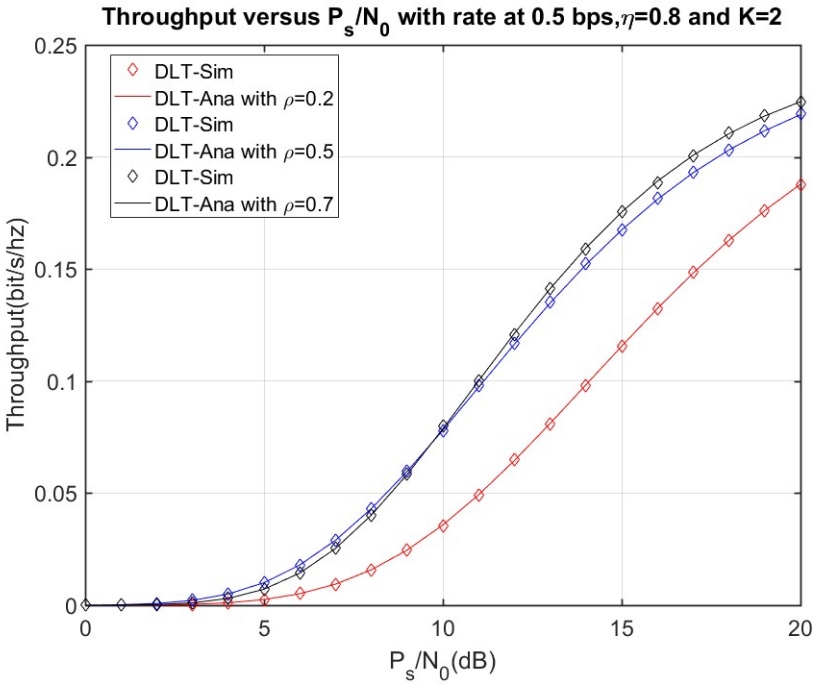

Figure 8. ST versus P_s/N_0 as η = 0.8, R = 0.5 bps K = 2 and ρ = 0.2, 0.5, 0.7.

4.2. Delay-Tolerant Transmission (DTT) Analysis

In Figure 9, the EC of the proposed system for DTT mode has a considerable increase with P_s/N_0 varies from 0 to 20 dB. Moreover, Figures 10 and 11 present the comparison of the system throughput between both DLT and DTT modes on the connection with K and ρ. The similarity with the above case, we set the main parameters as η = 0.8, R = 0.5 bps K = 2 and ρ = 0.2, 0.5, 0.7. It is clearly shown that the system throughput for DTT mode is better than for DLT mode when K varies from 0 to 10 and ρ from 0 to 1, respectively. The results indicate that all the simulation and analytical values are

agreed well with each other. Finally, Figures 12 and 13 show SER versus K and P_s/N_0, respectively. Then Figure 14 proposes the optimal power splitting factor versus P_s/N_0. In these Figs, the simulation results match tightly with analytical expressions in Section 3. Again, it can be formulated that less available power for EH in the interval of ρ smaller than the optimal ρ leads to less transmission power from the relay node and smaller values of throughput are observed at the destination node and has a larger outage probability.

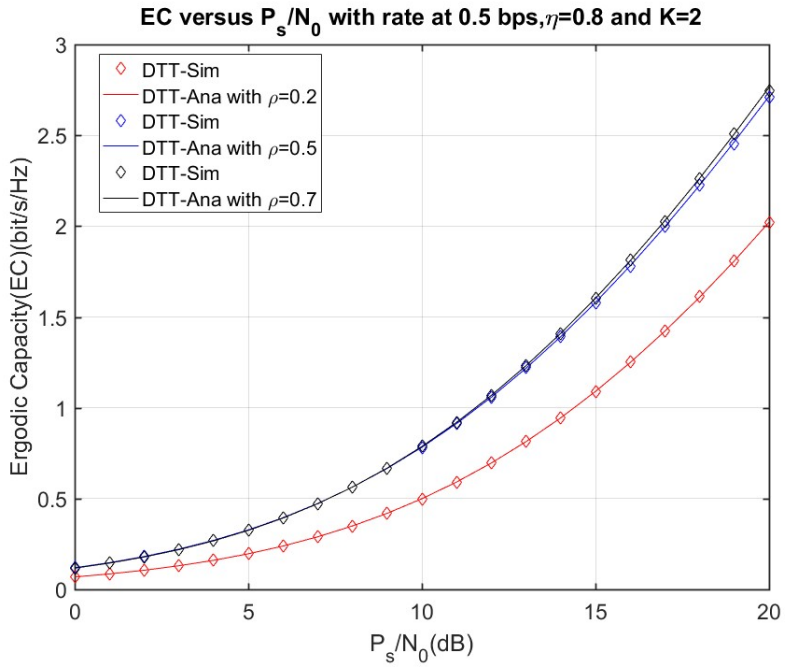

Figure 9. Ergodic Capacity (EC) versus P_s/N_0 as η = 0.8, R = 0.5 bps K = 2 and ρ = 0.2, 0.5, 0.7.

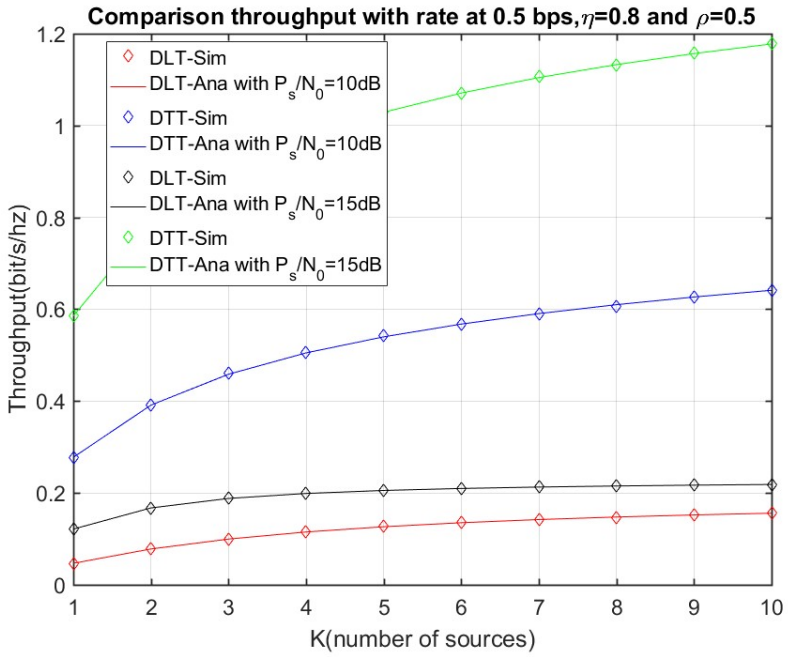

Figure 10. Comparison throughput of DLT and DTT modes versus K.

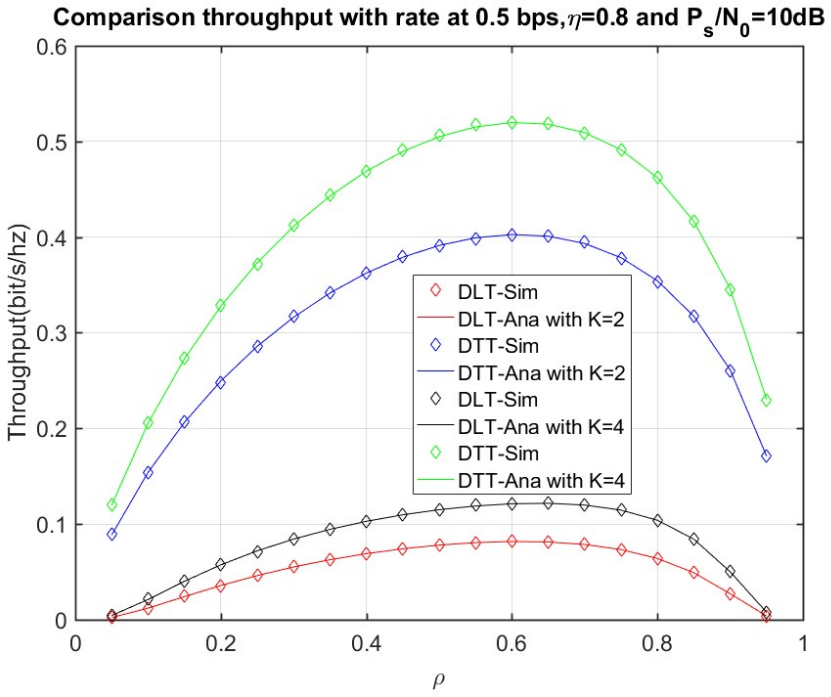

Figure 11. Comparison throughput of DLT and DTT modes versus ρ.

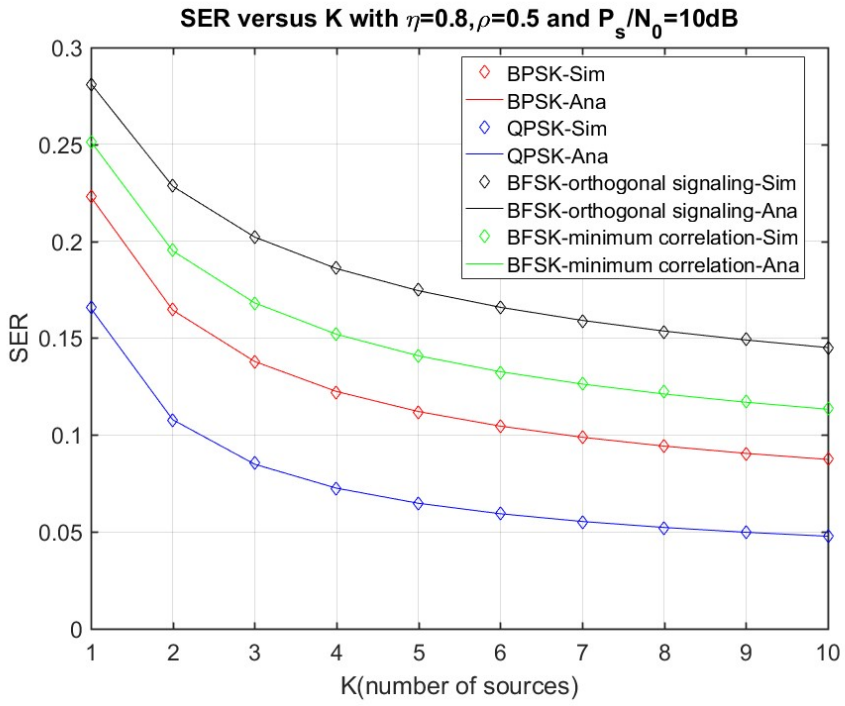

Figure 12. SER versus K.

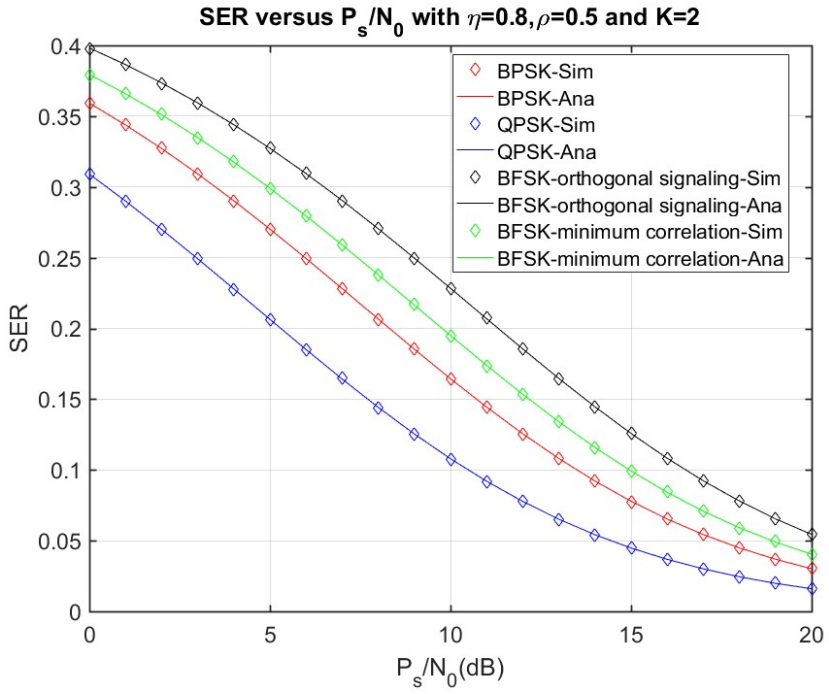

Figure 13. SER versus P_s/N_0.

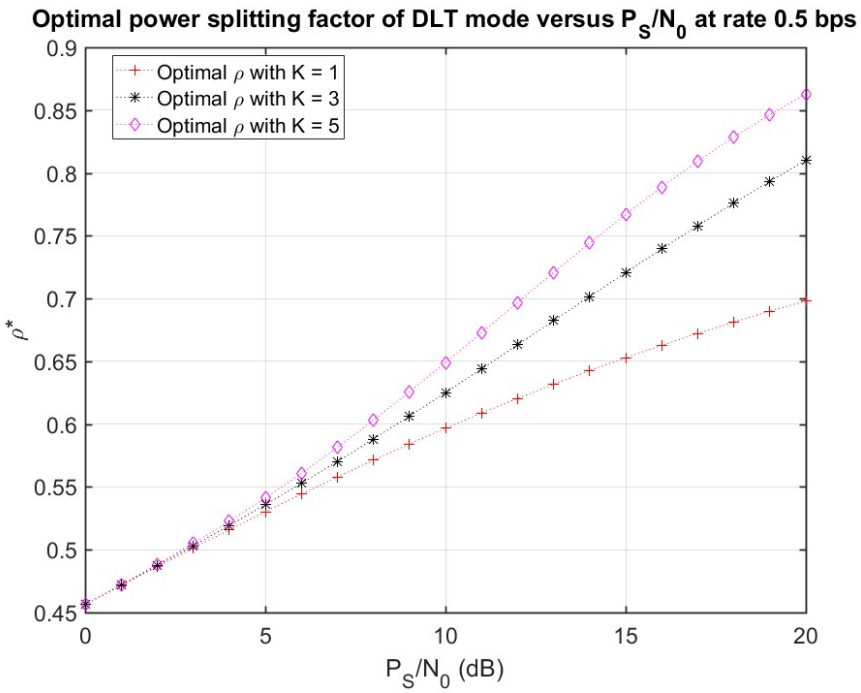

Figure 14. Optimal power splitting factor versus P_s/N_0.

5. Conclusions

In this paper, the SP analysis of multisource PS EH relaying network in the HD mode over a block Rayleigh-fading channel in both DLT and DTT modes is proposed and investigated. In the analysis process, we analyze and derive the CF expressions of the OP and ST in DLT mode and a CF expression for EC for DTT mode, respectively. Furthermore, we can obtain the CF for SER for DLT mode. After that, the optimal PS factor is investigated and derived in detail. Finally, the Monte Carlo simulation is used for validating the analytical analysis in connection with all system parameters.

The results show that the analytical and simulation results agree well with each other in connection with all system parameters. This solution can be considered as a novel recommendation for WPCN.

Author Contributions: T.N.N. and M.T. created the main idea, developed the performance evaluation by analysis and simulation and wrote the paper. T.-L.N. and D.-H.H. joined in the data analysis process. M.V. was working as the advisors of T.N.N. and M.T. to discuss and advise the main idea and performance analysis together.

Funding: This research was funded by the grant No. SP2018/59 and partially by No. LM2015070 of the Czech Ministry of Education, Youth and Sports.

Acknowledgments: This work was supported by the grant SGS reg. No. SP2018/59 conducted at VSB Technical University of Ostrava, Czech Republic and partly by The Ministry of Education, Youth and Sports from the Large Infrastructures for Research, Experimental Development, and Innovations project reg. No LM2015070.

Conflicts of Interest: The authors declare no conflict of interest.

References

1. Bi, S.; Ho, C.K.; Zhang, R. Wireless powered communication: Opportunities and challenges. *IEEE Commun. Mag.* **2015**, *53*, 117–125. [CrossRef]
2. Niyato, D.; Kim, D.I.; Maso, M.; Han, Z. Wireless Powered Communication Networks: Research Directions and Technological Approaches. *IEEE Wirel. Commun.* **2017**, 2–11. [CrossRef]
3. Yu, H.; Lee, H.; Jeon, H. What is 5G? Emerging 5G Mobile Services and Network Requirements. *Sustainability* **2017**, *9*, 1848. [CrossRef]
4. Rabie, K.M.; Salem, A.; Alsusa, E.; Alouini, M.S. Energy-harvesting in Cooperative AF Relaying Networks over Log-normal Fading Channels. In Proceedings of the 2016 IEEE International Conference on Communications (ICC), Kuala Lumpur, Malaysia, 23–27 May 2016.
5. Zhou, X.; Zhang, R.; Ho, C.K. Wireless Information and Power Transfer: Architecture Design and Rate-Energy Tradeoff. *IEEE Trans. Commun.* **2013**, *61*, 4754–4767. [CrossRef]
6. Bi, S.; Ho, C.K.; Zhang, R. Recent Advances in Joint Wireless Energy and Information Transfer. In Proceedings of the 2014 IEEE Information Theory Workshop (ITW2014), Hobart, Australia, 2–5 November 2014. [CrossRef]
7. Kawabata, H.; Ishibashi, K. RF Energy Powered Feedback-aided Cooperation. In Proceedings of the 2014 IEEE 25th Annual International Symposium on Personal, Indoor, and Mobile Radio Communication (PIMRC), Washington, DC, USA, 2–5 September 2014. [CrossRef]
8. Huang, K.; Lau, V.K. Enabling Wireless Power Transfer in Cellular Networks: Architecture, Modeling and Deployment. *IEEE Trans. Wirel. Commun.* **2014**, *13*, 902–912. [CrossRef]
9. Medepally, B.; Mehta, N.B. Voluntary Energy Harvesting Relays and Selection in Cooperative Wireless Networks. *IEEE Trans. Wirel. Commun.* **2010**, *9*, 3543–3553. [CrossRef]
10. De Rango, F.; Gerla, M.; Marano, S. A Scalable Routing Scheme with Group Motion Support in Large and Dense Wireless Ad Hoc Networks. *Comput. Electr. Eng.* **2006**, *32*, 224–240. [CrossRef]
11. Zhou, B.; Lee, Y.Z.; Gerla, M.; De Rango, F. Geo-LANMAR: A Scalable Routing Protocol for Ad Hoc Networks with Group Motion. *Wirel. Commun. Mob. Comput.* **2006**, *6*, 989–1002. [CrossRef]
12. Fazio, P.; De Rango, F.; Sottile, C.; Calafate, C. A New Channel Assignment Scheme for Interference-Aware Routing in Vehicular Networks. In Proceedings of the 2011 IEEE 73rd Vehicular Technology Conference (VTC Spring), Budapest, Hungary, 15–18 May 2011. [CrossRef]
13. Cassano, E.; Florio, F.; De Rango, F.; Marano, S. A Performance Comparison between ROC-RSSI and Trilateration Localization Techniques for WPAN Sensor Networks in a Real Outdoor Testbed. In Proceedings of the 2009 Wireless Telecommunications Symposium, Prague, Czech Republic, 22–24 April 2009. [CrossRef]
14. Zhou, X.; Zhang, R.; Ho, C.K. Wireless Information and Power Transfer: Architecture Design and Rate-energy Tradeoff. In Proceedings of the 2012 IEEE Global Communications Conference (GLOBECOM), Anaheim, CA, USA, 3–7 December 2012. [CrossRef]
15. Song, C.; Ling, C.; Park, J.; Clerckx, B. MIMO Broadcasting for Simultaneous Wireless Information and Power Transfer: Weighted MMSE Approaches. In Proceedings of the 2014 IEEE Globecom Workshops (GC Wkshps), Austin, TX, USA, 8–12 December 2014. [CrossRef]
16. Varshney, L.R. Transporting Information and Energy Simultaneously. In Proceedings of the 2008 IEEE International Symposium on Information Theory, Toronto, ON, Canada, 6–11 July 2008. [CrossRef]

17. Salari, S.; Kim, I.M.; Kim, D.I.; Chan, F. Joint EH Time Allocation and Distributed Beamforming in Interference-Limited Two-Way Networks With EH-Based Relays. *IEEE Trans. Wirel. Commun.* **2017**, *16*, 6395–6408. [CrossRef]
18. Liu, L.; Zhang, R.; Chua, K.C. Wireless Information and Power Transfer: A Dynamic Power Splitting Approach. *IEEE Trans. Commun.* **2013**, *61*, 3990–4001. [CrossRef]
19. Jameel, F.; Wyne, S.; Ding, Z. Secure Communications in Three-Step Two-Way Energy Harvesting DF Relaying. *IEEE Commun. Lett.* **2018**, *22*, 308–311. [CrossRef]
20. Chen, Y. Energy-Harvesting AF Relaying in the Presence of Interference and Nakagami-m Fading. *IEEE Trans. Wirel. Commun.* **2016**, *15*, 1008–1017. [CrossRef]
21. Nasir, A.A.; Zhou, X.; Durrani, S.; Kennedy, R.A. Relaying Protocols for Wireless Energy Harvesting and Information Processing. *IEEE Trans. Wirel. Commun.* **2013**, *12*, 3622–3636. [CrossRef]
22. Do, N.T.; Bao, V.N.; An, B. A Relay Selection Protocol for Wireless Energy Harvesting Relay Networks. In Proceedings of the 2015 International Conference on Advanced Technologies for Communications (ATC), Ho Chi Minh, Vietnam, 14–16 October 2015. [CrossRef]
23. Nguyen, S.Q.; Kong, H.Y. Generalized Diversity Combining of Energy Harvesting Multiple Antenna Relay Networks: Outage and Throughput Performance Analysis. *Ann. Telecommun.* **2016**, *71*, 265–277. [CrossRef]
24. Peng, C.; Li, F.; Liu, H. Optimal Power Splitting in Two-Way Decode-and-Forward Relay Networks. *IEEE Commun. Lett.* **2017**, *21*, 2009–2012. [CrossRef]
25. Men, J.; Ge, J.; Zhang, C.; Li, J. Joint Optimal Power Allocation and Relay Selection Scheme in Energy Harvesting Asymmetric Two-way Relaying System. *IET Commun.* **2015**, *9*, 1421–1426. [CrossRef]
26. Singh, S.; Modem, S.; Prakriya, S. Optimization of Cognitive Two-Way Networks with Energy Harvesting Relays. *IEEE Commun. Lett.* **2017**, *21*, 1381–1384. [CrossRef]
27. Cai, G.; Fang, Y.; Han, G.; Xu, J.; Chen, G. Design and Analysis of Relay-Selection Strategies for Two-Way Relay Network-Coded DCSK Systems. *IEEE Trans. Veh. Technol.* **2018**, *67*, 1258–1271. [CrossRef]
28. Kumar, N.; Bhatia, V. Outage Probability and Average Channel Capacity of Amplify-and-Forward in Conventional Cooperative Communication Networks over Rayleigh Fading Channels. *Wirel. Pers. Commun.* **2016**, *88*, 943–951. [CrossRef]
29. Bhatnagar, M.R. On the Capacity of Decode-and-Forward Relaying over Rician Fading Channels. *IEEE Commun. Lett.* **2013**, *17*, 1100–1103. [CrossRef]
30. Nguyen, T.; Quang Minh, T.; Tran, P.; Vozňák, M. Energy Harvesting over Rician Fading Channel: A Performance Analysis for Half-Duplex Bidirectional Sensor Networks under Hardware Impairments. *Sensors* **2018**, *18*, 1781. [CrossRef] [PubMed]
31. Nguyen, T.N.; Minh, T.H.; Tran, P.T.; Vozňák, M. Adaptive Energy Harvesting Relaying Protocol for Two-Way Half Duplex System Network over Rician Fading Channel. *Wirel. Commun. Mob. Comput.* **2018**. [CrossRef]
32. Nguyen, T.N.; Duy, T.T.; Luu, G.T.; Tran, P.T.; Vozňák, M. Energy Harvesting-based Spectrum Access with Incremental Cooperation, Relay Selection and Hardware Noises. *Radioengineering* **2017**, *26*, 240–250. [CrossRef]
33. *Table of Integrals, Series, and Products*; Academic Press: Cambridge, MA, USA, 2015. [CrossRef]
34. Abramovitz, M.; Stegun, I.A. *Handbook of Mathematical Functions:With Formulas, Graphs, and Mathematical Tables*; Dover Publications: New York, NY, USA, 1972.
35. McKay, M.R.; Grant, A.J.; Collings, I.B. Performance Analysis of MIMO-MRC in Double-Correlated Rayleigh Environments. *IEEE Trans. Commun.* **2007**, *55*, 497–507. [CrossRef]
36. Duong, T.Q.; Duy, T.T.; Matthaiou, M.; Tsiftsis, T.; Karagiannidis, G.K. Cognitive Cooperative Networks in Dual-hop Asymmetric Fading Channels. In Proceedings of the 2013 IEEE Global Communications Conference (GLOBECOM), Atlanta, GA, USA, 9–13 December 2013. [CrossRef]
37. Chong, E.K.; Zak, S.H. *An Introduction to Optimization*; John Wiley & Sons: Hoboken, NJ, USA, 2013.

© 2019 by the authors. Licensee MDPI, Basel, Switzerland. This article is an open access article distributed under the terms and conditions of the Creative Commons Attribution (CC BY) license (http://creativecommons.org/licenses/by/4.0/).